LA-UR-03-9160

Approved for public release;
distribution is unlimited.

Title:	ISOLATING TEMPORAL-DISCRETIZATION ERRORS FOR SEPARATE-VERIFICATION ANALYSES
Author(s):	Jerry S. Brock, Applied Physics Division
Date:	AIAA Aerospace Sciences Conference, January 2004

ISOLATING TEMPORAL-DISCRETIZATION ERRORS FOR SEPARATE-VERIFICATION ANALYSES

Jerry S. Brock*, Los Alamos National Laboratory, Los Alamos, NM 87545

Abstract

A novel type of numerical tool for separate-verification, a *verification controller*, is proposed and demonstrated. Verification controllers can ensure the accuracy and enhance the efficiency of separate time and space convergence studies by decoupling discretization errors. These supplemental tools are algebraic constraints on time-steps and grid-spacings that must be satisfied concurrent with the convergence-study simulations. Two verification controllers are presented: the discretization-error ratio (DER) and the convergence-power ratio (CPR). Temporal convergence studies are conducted and suggest that the CPR is more practical than time-steps or grid-spacing for the a-priori separation of discretization errors. The DER appeared to be a similarity variable for separate verification because all of the convergence histories coalesced onto a single error profile. The DER also implied a universal constant for decoupling errors; to accurately conduct separate verification analyses, the discretization errors must differ by at least one order-of-magnitude.

Introduction

Numerical solution methods for partial-differential equations (PDE) discretize continuum fields in time and space.[1,2] This finite approximation of a continuum embeds discretization errors into numerical simulations that are modeled in the PDE solver's error-ansatz equation. Verification analyses for PDE solvers, the study of their error-ansatz equation, should include time and space convergence studies. These computational studies, like all numerical PDE solutions, must be conducted in time and space asymptotic regimes wherein the numerical error is uniformly reduced as the discretization parameters are refined. The extent of each asymptotic regime and any relationship between these regimes, however, are not well defined prior to conducting numerical simulations. This report focuses on the specification of time-steps and grid-spacings so that separate time and space convergence studies are conducted in properly defined asymptotic regimes.

Convergence studies help confirm the computational implementation and theoretical foundation of numerical solution methods.[3-6] Convergence studies use the discretization error, the difference between computed and reference solutions, from multiple simulations to solve for parameters in the error-ansatz equation. The error model's unknowns are verification *metrics*[7]: convergence coefficients and rates. Convergence studies provide computational evidence of the functional properties postulated in the error-ansatz equation. If the simulation error is reduced under time-step and grid refinement, convergence studies also support the mathematical consistency of the numerical solver with the governing PDEs. For numerical solvers with many error sources, such as time and space discretization, there are at least two approaches to solving the error-ansatz equation: *simultaneous* and *separate* verification.

Simultaneous verification solves the original or *full*-ansatz equation wherein the total discretization error is modeled with time-step and grid-space dependent terms. Time and space verification metrics are computed concurrently by solving a system of non-linear, full-ansatz equations.[8] This solution, however, presents challenges: ambiguous initial condition specification together with potential multiple solutions, and the stability and expense of an iterative solution. In contrast, separate verification solves two *reduced*-ansatz equations that are obtained by partitioning the total discretization-error model into time-step and grid-space dependent segments. Time and space metrics are computed individually by solving both of these error models. Reduced-ansatz equations possess an efficient, closed-form analytical solution since they model each discretization-error source with one simple term.

The accuracy of separate verification analyses is predicated on obtaining a single-source discretization error; each reduced-ansatz equation *defines* the total simulation error as wholly either time or space error. Prescribing simulation series to isolate a single source of discretization error, however, is problematic. The only measurable discretization error is the total value, which generally includes both time and space components. Separating two sources of independent discretization error could be straightforward using the full-ansatz equation if estimates of each verification metric were known. Unfortunately, while convergence rates may be predicted, convergence coefficients, scaling products proportional to solution derivatives, are generally not known a-priori to any simulation.

*Member AIAA. LANL Technical Staff Member.

This document is also available as Los Alamos National Laboratory Technical Report LA-UR-03-9160 December 2003.

The goal of this effort is to ensure the accuracy and enhance the efficiency of separate-verification analyses. This analysis approach involves conducting separate time and space convergence studies, and is prevalent in the literature for verification of numerical PDE solvers. Indeed, independent discretization-error models are frequently confirmed by modified-equation analysis, the formal derivation of error-ansatz equations.[9-11] For numerical methods without derived error models, separate verification provides an estimate of verification metrics and evaluation of error-model assumptions. Separate verification also provides an initial approach for verifying coupled-physics simulators that combine disparate PDE solvers. These simulators solve for numerous continuum fields whose discretization variables, including time and space, each represent a potential reduced-ansatz equation. The metrics obtained by solving reduced-ansatz equations, however, are not guaranteed to be accurate; no formal mechanism exists to a-priori decouple discretization errors.

This report proposes a novel, supplemental tool for separate-verification analyses: *verification controllers*. These numerical tools are algebraic constraints relating time-steps and grid-spacings, which must be satisfied concurrent with convergence-study simulations. Verification controllers are based upon the full-ansatz equation, and decouple independent discretization errors by estimating when they contribute equally to the total simulation error. When combined with heuristic data about maximum allowable time-steps and grid-spacing, both extents of a *separate*-asymptotic regime may be predicted. Separate-asymptotic regimes are the desired regions wherein the simulation error is dominated by a single source of error. The ability to focus on a single source of discretization error would guarantee the consistency of computed errors with the reduced-ansatz equation and, thus, ensures the accuracy of separate verification. Furthermore, well prescribed simulation series enhance the efficiency of separate verification analyses; convergence studies would require a minimum number of simulations because their computed solutions would fall within separate-asymptotic regimes.

This report continues with a brief description of the ansatz equation comprised of independent time and space discretization errors. The separate-verification method is then outlined, including the equations used to compute metrics. The mathematical and operational requirements for accurately solving reduced-ansatz equations are then discussed, followed by development of verification controllers. A temporal convergence study of a common PDE solver, one that can produce comparable time and space discretization error, is then presented. A summary concludes this document.

Separate-Verification Analysis

Separate-verification analysis of numerical solvers is widely applicable because reduced-ansatz equations can model various discretization-error sources. This report is focused on temporal and spatial verification because discrete time and space approximations are common sources of error within numerical PDE solvers.

Error Ansatz

Separate-verification analysis of numerical solution methods is predicated on the generation of independent discretization errors. For numerical PDE solvers, the total discretization error, E_{total}, may be modeled as the summation of independent spatial, E_s, and temporal, E_t, components as presented in Equation 1.

$$E_{total} = E_s + E_t \tag{1}$$

Modeling discretization errors generated by PDE solvers as mathematically independent is often confirmed by modified-equation analysis.[9-11] This technique derives error-ansatz equations by substituting solution variables in discrete equations with Taylor's series expansions. The analysis' objective is to recover the original, continuum PDE together with remainder terms that define the truncation error. The lowest-order of these additional terms generally comprise the error model, and they are explicit functions of the space and time discretization parameters: the grid-spacing, Δx, and time-step, Δt. Independent space and time errors are then modelled as $E_s \approx A(\Delta x)^p$ and $E_t \approx B(\Delta t)^q$. An error-ansatz equation comprised solely of these two terms is presented in Equation 2.

$$E_{total} \approx A(\Delta x)^p + B(\Delta t)^q \tag{2}$$

The numerical method's order-of-accuracy, the rate at which computed solutions converge to the continuum solution under grid and time-step refinement, is set by the space and time convergence rates, p and q. The convergence coefficients, A and B, are proportional to suitably averaged spatial and temporal solution derivatives, whose order of differentiation is set by the accuracy of the spatial-operators and time-integrators used in the numerical solver. Moreover, convergence coefficients are a measure of the component spatial and temporal discretization error. Their relative magnitude, which is not known a-priori to any simulation, suggests which component may dominate the total error.

Verification Metrics

A primary goal of verification analyses is evaluating convergence rates. Separate convergence studies focus on individual error sources, and provide an operational convenience for computing verification metrics.

The remainder of this report, unless otherwise noted, will focus on temporal-verification analysis. All further developments and discussion, however, are equally valid for separate-spatial verification. When E_{total} is wholly comprised of temporal-discretization error, then Equations 1 and 2 can be simplified into the temporal reduced-ansatz equation as presented in Equation 3.

$$E_{total} \approx E_t \approx B(\Delta t)^q \tag{3}$$

For verification analyses, the total discretization error is defined as the difference between computed, ζ, and reference, ζ^*, solutions, and it is often measured using a function norm: $\|\zeta - \zeta^*\|$. If E_{total} is measured using norms and any source of error may dominate the total error, then $A \geq 0$ and $B \geq 0$. Two evaluations of Equation 3 and, thus, two numerical simulations are required to compute both temporal-verification metrics: q and B. These simulations are conducted using unique 'coarse' and 'fine' time-steps, Δt_c and Δt_f, and generate two corresponding, unique total discretization errors: $\zeta_c - \zeta^*$ and $\zeta_f - \zeta^*$. The solution of Equation 3 is then straightforward. The temporal-convergence rate, q, is often computed first by the quotient in Equation 4.

$$q = \frac{\log(\| \zeta_c - \zeta^* \| / \| \zeta_f - \zeta^* \|)}{\log(\Delta t_c / \Delta t_f)} \tag{4}$$

In Equation 3, either combination of coarse or fine time-step and error-norm can then be used to compute B. The temporal-convergence coefficient, B, may then be computed as presented in Equation 5.

$$B = \| \zeta_c - \zeta^* \| / (\Delta t_c)^q \tag{5}$$

Equations 4 and 5 represent a simple, robust method for solving the temporal reduced-ansatz equation. These solution equations are also easily adapted for computing verification metrics for other discretization-error sources that are modeled similar to Equation 3.

Separate Asymptotic Regimes

An important, but often overlooked, objective of convergence studies is to confirm that the verification metrics are relatively constant in the asymptotic regime. No formal criterion exists or is offered herein to gauge the relative constancy of metrics. Instead, the use of verification controllers to prescribe asymptotic regimes represents a first-step towards making that subjective determination about constant verification metrics.

Obtaining sufficiently steady verification metrics is important for many reasons. Only steady convergence rates, as determined by the analyst, can be compared to theoretical predictions. If the convergence rate is not steady then the discretization error may become unbound, which implies that the numerical solver is inconsistent with the governing equations. Unsteady verification metrics also suggest that the error-ansatz might not properly characterize the discretization error, and an alternative model may be necessary. Conversely, sufficiently steady verification metrics imply that the ansatz equation is an appropriate error model and that the convergence study was conducted in an asymptotic regime. For separate verification, steady metrics confirm that the reduced-ansatz equations correctly model independent discretization errors.

The challenge of obtaining steady verification metrics stems from the approximations inherent to error models. Error-ansatz equations are models imposed upon the convergence data. This imposition is necessary because the formal derivation of truncation error is not always possible, particularly for complex numerical PDE solvers applied to general problems. Inclusion of all of the truncation error's terms in the error-ansatz equation would also not be practical. The form of the error-ansatz equations, however, are guided by truncation-error analysis; generally, both error equations contain scaled, power-law terms with respect to Δx and Δt.

An important difference between truncation-error and error-ansatz equations is variability of their parameters. Since truncation error is derived from Taylor's series, its coefficients and exponents are constant. In contrast, an error-ansatz approximates or models discretization error since it retains or assumes only the lowest-order terms of the truncation error. The coefficients and exponents of the error-ansatz equation, the verification metrics, could then not be expected to also be constant. Indeed, verification-metric variability may partially expose the simplification of the error-ansatz from the truncation-error equation. While it is important to assess whether convergence studies are conducted within asymptotic regimes, and that assessment is often gauged by whether the metrics are relatively constant, a formal criterion for measuring or assessing that variability does not exist.

An approach that is currently used to ascertain steady verification metrics can also simultaneously, but only partially, characterize asymptotic regimes. This heuristic method generates a surplus number of simulations to solve Equation 3. Using these simulations, multiple sets of metrics are computed and compared. If the metric sets are relatively constant then the convergence study was conducted within a separate-asymptotic regime, and the metrics reported are often an average of those already found. If the metrics are not sufficiently steady then additional simulations, with succeedingly refined discretization parameters, are conducted until the

newly-found metrics converge. Using discretization parameters from this final, expanded simulation series to define a portion of the asymptotic regime is then possible but superfluous; steady metrics have already been obtained. Convergence studies for separate verification, therefore, are generally iterative and only completed when the metrics are sufficiently steady.

Once steady metrics are found, one essential criterion of verification analysis is the comparison of computed and predicted convergence rates. If these rates match, this provides evidence that the software has faithfully implemented the numerical solver. Failure of the convergence rates to match may be caused by many factors including error-modeling assumptions. For separate verification, the independence of error sources must be confirmed. The discretization error used to solve reduced-ansatz equations must be *pure*; it must be produced by a single error source. If the error is not pure, then any metric obtained through separate verification is not accurate as defined by reduced-ansatz equations and, thus, they are not valid for verification.

Verification controllers are designed to ensure that reduced-ansatz equations are solved with pure discretization error. This guarantee would eliminate any doubt about the accuracy of separate-verification analyses if computed convergence rates fail to match predicted values. The list of subsequent analyses would then be narrowed to include a more complex error model for verification, or an intensive investigation of the numerical solver. Pure discretization error is only produced within separate-asymptotic regimes. As described above, the prevalent approach to separate verification does partially define these regimes after obtaining steady metrics, but only extraneously. An alternative methodology, adopted in this effort, reverses this process: first define a separate-asymptotic regime, then compute steady, accurate verification metrics.

Throughout the remainder of this report, steady verification metrics will refer to sufficiently constant convergence coefficients and rates unless indicated

Operational Requirements for Separate Verification

Mathematical and operational requirements exist for separate-verification. The mathematical requirements, reflected in Equations 1 and 2, include the independence of error-model terms. Equally important are two operational requirements. First, the time-steps and grid-spacing used for verification must ensure mathematical consistency between the discrete and continuum variants of the governing equations. Second, unique sets of Δt and Δx must elicit separately the errors defined in the time and space reduced-ansatz equations.

Separate Temporal Verification

An idealized error profile for separate-temporal verification is presented in Figure 1. This convergence history is plotted as the total numerical error verses the time-step. In order to minimize computational expense, temporal convergence studies usually progress from larger to smaller time-steps. The *start* of the temporal asymptotic regime is on the right-hand-side of Figure 1. For time-steps below the maximum allowable value, Δt_{max}, there are two distinct segments of the error profile. Initially, temporal discretization error dominates the total error. When $E_{total} \approx E_t$, the slope of the error profile on a logarithmic scale is, q, the temporal-convergence rate. This region is the separate-temporal asymptotic regime. The *exit* of this regime is indicated by the minimum allowable time-step, Δt_{min}. As the time-step is further refined, E_t is reduced and spatial error dominants the total error: $E_{total} \approx E_s$.

While each convergence-profile segment in Figure 1 corresponds to individual, dominant error sources, both errors exist in numerical PDE simulations. The dashed lines in Figure 1 are a continuation of the variable-temporal and constant-spatial components of the total numerical error. Since both E_t and E_s exist, then the time-step and grid-spacing must fall in their respective asymptotic regimes. For numerical PDE solvers to achieve mathematical consistency, not only should $\Delta t \le \Delta t_{max}$, but Δx must also be within the spatial asymptotic regime. The maximum allowable grid-spacing, Δx_{max}, would be available from the required, concurrent spatial convergence study. In Figure 1, the

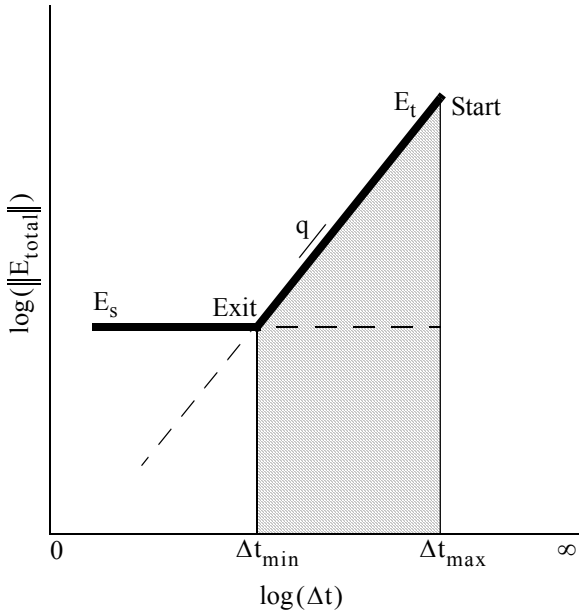

Figure 1: Temporal Convergence History With Constant Spatial Discretization Error; Total Error vs. Time-Step.

full-ansatz equation is valid for all time-steps below Δt_{max} if $\Delta x \le \Delta x_{max}$. The accurate solution of the temporal reduced-ansatz equation, however, is restricted to the shaded region between Δt_{max} and Δt_{min}, but $\Delta x \le \Delta x_{max}$ must also be satisfied.

Accurately solving reduced-ansatz equations requires well defined, wide asymptotic regimes. For separate-temporal verification, numerous simulations may be required to ascertain converged metrics and establish Δt_{max}. If the steady convergence rate does not match the predicted value, however, separate verification's existing approach offers no guidance as to whether the error was not pure below Δt_{max} or that the original error model is inadequate. Eliciting pure temporal error may be possible by suppressing the spatial error; in Figure 1, lowering E_s would reduce Δt_{min} and, thus, widen the separate-temporal asymptotic regime. The grid-spacing corresponding to a reduced E_s, possibly below Δx_{max}, might increase the convergence study's computational expense, but this operational restriction may be necessary for separate-temporal verification.

Verification Controllers

Separating time and space discretization errors for verification analyses is predicated upon the ability to first determine when they are equivalent: $E_s \approx E_t$. If this relationship was modeled using Δt and Δx as independent variables, then these parameters could be manipulated to alternately suppress one error source and expose the other error. This equivalence model, together with limiting constants, could then be a time-step, grid-space controller for separate verification analyses, or as succinctly termed herein a *verification controller.*

Discretization-Error Ratio (DER)

Simplifying the total discretization-error model into the temporal reduced-ansatz equation is only possible if $E_s \ll E_t$. This suggests defining a verification controller as the quotient of discretization errors, termed herein a discretization-error ratio (DER). One option for defining this quotient would place the minimized error in the numerator and the verification analyses' objective error in the denominator. Separate temporal and spatial verification analyses then require reciprocal error ratios. Each DER is identified herein by the quotient's numerator. Using this nomenclature, separate-temporal verification uses the spatial discretization-error ratio, DER_s, which is defined in Equation 6.

$$DER_s = \frac{E_s}{E_t} \approx \frac{A(\Delta x)^p}{B(\Delta t)^q} \qquad (6)$$

The DER_s directly relates discretization errors; when E_s and E_t are comparable $DER_s \approx 1$. In Figure 1, $E_s \approx E_t$ corresponds to a pivotal time-step; the total discretization error is dominated by a single error source on either side of Δt_{min}. When the spatial error dominates the temporal error, $E_s \gg E_t$, the DER_s is much greater than unity, $DER_s \gg 1$, and $\Delta t \le \Delta t_{min}$. Conversely, when the temporal error dominates the spatial error, $E_s \ll E_t$, the DER_s is much less than one, $DER_s \ll 1$, and $\Delta t \ge \Delta t_{min}$. While verification metrics serve as constants in Equation 6, Δt and Δx are the independent variables of the DER_s.

As independent variables, Δx and Δt may exhibit weak problem dependencies because time-steps and grid-spacings are often selected according to important simulation features, e.g. solution gradients. In contrast, Δt_{min} and Δt_{max}, the two discretization parameters that bound separate-temporal asymptotic regimes, are algorithm and problem dependent. For example, the regime's exit occurs when $E_s \approx E_t$, or as modeled herein when $A(\Delta x)^p \approx B(\Delta t_{min})^q$. As functionally related to convergence coefficients and rates, Δt_{min} is, therefore, algorithm and problem dependent. The time-step that defines a separate-temporal asymptotic regime's start is similarly dependent as reflected by the necessarily heuristic search for Δt_{max} conducted concurrent to temporal convergence studies.

Verification controllers offer an alternative, indirect measure of separate asymptotic regimes. For example, instead of directly using Δt_{min} and Δt_{max} to define a temporal asymptotic regime, a pair of DER_s values could define the regime's extent. The regime's bounding time-steps could then be quantified using Equation 6. Moreover, a verification-controller's regime-bounding limits may offer reduced algorithm and problem dependencies relative to Δx or Δt. By abstracting a regime's extent from discretization parameters to relationships between the error components, verification controllers generalize the definition of separate asymptotic regimes. Verification-controller limits may then be more easily obtained and even constant under certain conditions and, thus, more widely applicable.

The present objective is to define separate-temporal asymptotic regimes without one or both of the algorithm and problem dependencies of Δt_{min} and Δt_{max}. The most important of these time-steps is Δt_{min}. For any grid-spacing, Equation 6 infers that Δt_{min} corresponds to the maximum spatial discretization-error ratio: $DER_{s,\,max}$. As discussed below, $DER_{s,\,max}$ is known prior to conducting convergence studies. In contrast, there exists no known, *non-zero* value for $DER_{s,\,min}$, which corresponds to Δt_{max}. While a separate-temporal asymptotic regime is defined by $DER_s = E_s / E_t \ll 1$, a null value for $DER_{s,\,min}$ is not relevant; if $DER_s = 0$

then $E_s = 0$ and there is no need to separate time and space errors. The $DER_{s,max}$, together with other heuristic information about Δt_{max}, then effectively define a separate-temporal asymptotic regime.

Within a separate-temporal asymptotic regime $DER_s = E_s/E_t \ll 1$. Unity, however, is not a proper value for $DER_{s,max}$; this limit would not guarantee pure temporal discretization error. Postulate instead that to confidently attribute the total discretization error to a single error source, the minimized error must be at least one order-of-magnitude smaller than the objective error. For separate-temporal verification then $E_s \le (10^{-1})E_t$ and $DER_{s,max}$ would be replaced by the generalized limit DER_{max}. As a direct comparison of discretization errors, expressed as a non-dimensional quotient, the DER_s incorporates all pertinent information for verification controllers; the DER_{max} may then be a universal constant for separate verification.

Implicit in the above premise is that the DER is a *similarity variable* for separate verification. If the total discretization error were plotted verses this quotient, all convergence profiles would coalesce onto one profile. More important for this effort, the DER_{max} would be devoid of algorithm and problem dependencies and, thus, broadly applicable in defining separate asymptotic regimes. The DER_s bounds, together with a proposed limiting constant, are presented in Equation 7.

$$DER_{s,min} \le DER_s \le DER_{max} \approx 10^{-1} \qquad (7)$$

The DER_s is an obvious, straightforward candidate for separating time and space discretization errors. Equation 6, however, cannot be used to a-priori separate these errors because convergence coefficients are not known prior to conducting simulations. The most important feature of the DER_s is the functionality modeled in Equation 6; the efficacy of a numerical solution method to reduce component discretization errors is embodied in the products $(\Delta t)^q$ and $(\Delta x)^p$ termed herein *convergence powers*.

Convergence-Power Ratio (CPR)

Another verification controller, the convergence-power ratio (CPR), compares the efficacy of a numerical solver to reduce component discretization errors. The CPR is a non-dimensional quotient of convergence powers; the minimized error's convergence power is in the numerator and the objective error's convergence power is in the denominator. Separate temporal and spatial verification then require reciprocal convergence-power ratios. Each CPR is identified herein by the quotient's numerator. Separate-temporal verification then uses the spatial convergence-power ratio, CPR_s, which is defined in Equation 8.

$$CPR_s = \frac{(\Delta x')^p}{(\Delta t')^q} = \frac{(\Delta x/L)^p}{(\Delta t/T)^q} \qquad (8)$$

Equation 8 uses two non-dimensional discretization parameters: $\Delta x' = \Delta x/L$ and $\Delta t' = \Delta t/T$. The time and length scales, T and L, may be arbitrarily set but they often reflect important simulation features.

An idealized error profile for separate-temporal verification, plotted as the total numerical error verses the CPR_s, is presented in Figure 2. In order for Figures 1 and 2 to correspond, the abscissa in Figure 2 is reversed. For constant grid-spacing, Equation 8 is minimized when the time-step is relatively large so the $CPR_{s,min}$ corresponds to the asymptotic regime's start at Δt_{max}. Conversely, $CPR_{s,max}$ corresponds to the regime's exit at Δt_{min}. In Figure 2, the slope of the separate-temporal regime on a logarithmic scale is -1. This slope is identical for all integrators regardless of their temporal convergence rate as a consequence of including $(\Delta t)^q$ in the denominator of the CPR_s,

As implied within Figure 2, the extent of a separate-temporal asymptotic regime can be set by $CPR_{s,min}$ and $CPR_{s,max}$. The corresponding time-steps, Δt_{max} and Δt_{min}, could then be computed using Equation 8. This procedure relies upon knowing the convergence rates, T and L prior to the convergence study. This procedure also requires that both CPR_s limits are known. As functionally dependent upon Δt_{max}, the

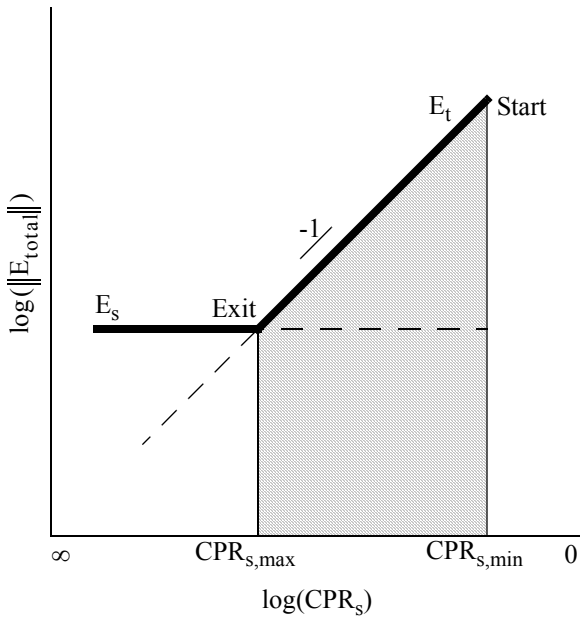

Figure 2: Temporal Convergence History With Constant Spatial Discretization Error; Total Error vs. CPR_s.

$CPR_{s,\,min}$ is algorithm and problem dependent; it must then be found iteratively within the temporal convergence study. This renders the $CPR_{s,\,min}$ superfluous to the a-priori specification of asymptotic regimes. The $CPR_{s,\,max}$, together with other heuristic information about Δt_{max}, then effectively define the full extent of a separate-temporal asymptotic regime. The CPR_s bounds are presented in Equation 9.

$$CPR_{s,\,min} \le CPR_s \le CPR_{s,\,max} \tag{9}$$

While the DER_{max} may be a universal constant for separate verification, the $CPR_{s,\,max}$ is not easily postulated. The limit $CPR_{s,\,max}$, however, can be determined through computational experiments. Graphical methods for determining the $CPR_{s,\,max}$ and DER_{max} are demonstrated later in this report.

Contrasting Verification Controllers

Verification controllers are *conceptually distinguished* by the types of terms used to compare error sources. A straightforward controller would compare discretization errors directly as this is necessary to simplify full-ansatz equations. The DER embodies this comparison and intrinsically provides a universal constant, DER_{max}, for separating errors. The DER, however, cannot be used to a-priori specify Δt and Δx for separate convergence studies as it includes solution-dependent convergence coefficients. In contrast, the CPR reduces solution dependencies by not including A and B, but it does not directly compare discretization errors. Instead, the CPR compares the potential to reduce errors under time-step or grid-spacing refinement.

Verification controllers are *procedurally distinguished* by their implementation and versatility within separate convergence studies. Using the DER requires that A and B are known prior to conducting the convergence study, but these constants are unknown for any particular simulation. Convergence coefficients are also solution dependent which precludes their reuse in subsequent verification analyses of other problems. Simultaneously solving reduced-ansatz equations and satisfying the DER is then a heuristic, iterative procedure. While the DER_{max} is valid for all separate-verification analyses, using Equation 6 to quantify time-steps that bound separate-temporal asymptotic regimes is limited to a single convergence study.

In contrast, the CPR can be used non-iteratively for separate-verification. The constants in Equation 8 are known prior to conducting convergence studies. Using this equation, any value of $CPR_{s,\,max}$ is then sufficient to predict Δt_{min} for any grid-spacing. The non-iterative implementation procedure afforded by the CPR is essential for the practical use of verification controllers.

Asymptotic Regime Time-Steps

As discussed above, of the two verification controllers proposed, only the CPR_s can be used to a-priori separate discretization errors. For separate-temporal convergence studies, Δt_{max} and the $CPR_{s,\,max}$ bound the asymptotic regime. While Δt_{max} is found within the convergence study, the $CPR_{s,\,max}$ must be known before conducting the study's simulations. This verification-controller limit indirectly determines the minimum time-step Δt_{min}. The relationship between $CPR_{s,\,max}$ and Δt_{min} is presented in Equation 10.

$$CPR_{s,\,max} = \frac{(\Delta x/L)^p}{(\Delta t_{min}/T)^q} \tag{10}$$

The use of Equation 10 to predict the error-decoupling time-step is straightforward. For any grid-spacing, an equation for Δt_{min} is presented in Equation 11, where all of the variables are known including $CPR_{s,\,max}$.

$$\Delta t_{min} = T\,(CPR_{s,\,max})^{-1/q}\,(\Delta x/L)^{p/q} \tag{11}$$

The remainder of this report will include using the CPR_s to predict time-steps to decouple time and space errors. Convergence studies will then be conducted to assess the accuracy of these predictions. Moreover, the basic concepts underlying both the CPR_s and DER_s verification controllers will also be examined.

Demonstration Problem

To assess the theoretical concepts and practical utility of verification controllers, a demonstration problem must satisfy various requirements. First, the numerical solver must produce time and space discretization errors of comparable magnitude. Second, a full error profile, with distinct time and space-dominant regions similar to Figures 1 and 2, is required to identify the simulation parameters when the errors are equivalent. Verification controller limits are then extracted from the asymptotic regime's exit. This method may be relatively expensive computationally and requires a reference solution, but it is straightforward and requires few assumptions.

Governing Equations

The equation selected for this demonstration effort governs the one-dimensional advection of a particle within a velocity field. For this problem, the rate-of-change of the particle's position, x_p, is equal to the velocity function, $u(x_p)$, as presented in Equation 12.

$$dx_p/dt = u(x_p) \tag{12}$$

Particle advection may be modeled as an autonomous equation that is valid for steady or time-variant velocity functions.[12] In Equation 12, the variable 't' can then

represent either time or the distance along the integration pathline. The discrete solution of Equation 12 entwines two distinct numerical techniques, each of which imparts discretization errors into the simulation.

Spatial discretization error was incurred by mapping velocities from a grid onto the particle through piece-wise, cell-based interpolation. One-dimensional space is often discretized into line-elements wherein linear functions are used for isoparametric interpolation, i.e. transforming the spatial coordinates and reconstructing discretized continuum data.[13] Spatial transformation involves mapping the cell's geometry from a physical, x, to a cell-based coordinate system, where $\xi \in [0, 1]$. Interpolation produces an approximate but continuous mapping of discrete data, stored at cell-vertices (cv), $\bar{x}^{cv}$, to the cell's interior. If the discrete-field data are exact, $\bar{u}^{cv} = u(\bar{x}^{cv})$, then the original continuum field, $u(x)$, is modeled as the interpolant, $u(\xi, \bar{u}^{cv})$, and a discretization error as presented in Equation 13.

$$u(x) = u(\xi, \bar{u}^{cv}) + O(\Delta x^2) \tag{13}$$

Equation 13 indicates that interpolation incurs a discretization error. For linear interpolation, this error is avoided if $u(x)$ is also linear. Conversely, when $u(x)$ is non-linear, the spatial error is second-order, $O(\Delta x^2)$, where Δx is a cell width. The semi-discrete governing equation substitutes the continuous velocity function with the reconstruction field as shown in Equation 14.

$$dx_p/dt = u(\xi_p, \bar{u}^{cv}) \tag{14}$$

Temporal or time-stepping discretization error was incurred in this demonstration problem by using explicit Runge-Kutta integrators to solve Equation 14. The combination of time integration and spatial interpolation formed the fully-discrete governing equation.

Velocity Field

Another requirement for the demonstration problem was to ensure sufficient terms within the error-ansatz, i.e., the integrator and interpolant should not provide the exact solution. A non-linear, infinitely differentiable sinusoidal velocity was used to satisfy this requirement. Furthermore, the particle must not traverse through a stagnation point where it would become trapped; if $u(x) = 0$ then Equations 12 and 14 dictate that $x_p(t)$ becomes invariant. Herein, the velocity did not change sign; for all $t \geq 0$, $u(x) > 0$ was guaranteed.

The velocity field is shown in Equation 15, where the constants represent the wave amplitude, $a = 2$, the average velocity, $b = 2.75$, and wavelength, $\lambda = 5$.

$$u(x) = a \sin(2\pi x/\lambda) + b \tag{15}$$

Exact Solution

The continuous formulation of the governing equation is comprised of Equations 12 and 15. The exact solution of these equations, including the particle's initial position, $x_0 = x_p(t = 0)$, and conditioned on $|b| > |a|$, is presented in Equation 16 where $c^2 = b^2 - a^2$.

$$x_p(t) = \frac{\lambda}{\pi} \operatorname{atan}\left\{\left(\frac{c}{b}\right)\tan\left[\operatorname{atan}\left(\frac{(b)\tan(\pi x_0/\lambda) + a}{c}\right) + \left(\frac{\pi c}{\lambda}\right) t\right] - \frac{a}{b}\right\} \tag{16}$$

Simulation Parameters

The spatial domain, $x \in [0, L]$ where $L = 16$, was sufficiently long to contain at least three wave forms. Equal grid spacings were used for each simulation, where $\Delta x = L/N_c$ and N_c is the number of cells. Three grid resolutions where chosen for the temporal convergence studies: $N_c = 160, 480$ and 1600. During the time integration, where $t \in [0, T]$ and $T = 5$, the particle moved through about two wavelengths. Constant time-steps were used, where $\Delta t = T/N_t$ and N_t is the number of time-steps. Finally, the only simulation parameter not specified above is Δt, the independent variable for temporal convergence studies.

Results and Discussion

The semi-discrete form of the demonstration problem, Equation 14, was solved using five explicit Runge-Kutta integrators[12]: the first-order or Euler's method, mid-point and trapezoidal second-order methods (RK2_Mid and RK2_Trap), a third-order method (RK3) and a fourth-order method (RK4). For each integrator, temporal convergence studies were conducted for the three prescribed grids. For the fifteen convergence studies, the discretization error was measured using the L_1, L_2 and L_∞ norms.[7] The error profiles presented below are limited to the L_∞ norm. For this smooth problem, however, these error profiles are similar to those obtained using the other norms. The following results also focus on the finest grid resolution, $N_c = 1600$, because they are characteristic of the error profiles obtained with each grid. This limited but representative set of convergence profiles is used below to evaluate the two proposed verification controllers.

One objective for this effort is to assess verification controllers, which includes obtaining $CPR_{s,\max}$ and confirming the ability of Equation 11 to predict Δt_{min}. Table 1 presents the maximum CPR_s values and the corresponding time-steps for each integrator from a previous version of this temporal convergence study.[14] These parameters are indicated in the remaining figures.

Integrator	$CPR_{s,\,max}$	Δt_{min}
Euler	0.012	1.63×10^{-4}
RK2_Mid & Trap	0.063	1.25×10^{-2}
RK3	0.29	5.52×10^{-2}
RK4	1.4	1.15×10^{-1}

Table 1: Verification-Controller Limits and Time-Steps to Separate Discretization Errors; $N_c = 1600$.

Five temporal convergence profiles, plotted as the total numerical error verses the time-step, are presented in Figure 3, one for each of the integrators. Numerous simulations were conducted for each integrator to characterize the error profiles. The two second-order integrators produce nearly identical error profiles, and so they are considered collectively in this discussion. Within this logarithmic plot, the slope of each error profile above Δt_{min}, either one, two, three or four, matches the desired convergence rate and, thus, verifies each integrator. As the time-step is refined, the error profiles asymptote to the identical, constant spatial error because the grid is held fixed for these simulations.

As discussed previously, Figure 3 is the typical format for presenting temporal convergence profiles. Indeed, inspecting error-profile slopes, which are convergence rates, is the graphical representation of solving reduced-ansatz equations. Figure 3 also demonstrates the difficulty in using time-steps to prescribe asymptotic regimes. While Δt_{max} is nearly coincident at the start of each regime, Δt_{min} and the regime's extent differ for each integrator. Unfortunately, when using time-steps to ensure pure temporal error, Δt_{min} is most important. These results, together with inferences from the full-ansatz equation, suggest that time-steps are not practical for the a-priori separation of discretization errors; the time-steps that define an asymptotic regime's bounds and extent are algorithm and problem dependent.

The convergence profiles of this problem are different than the one idealized in Figure 1. As shown in Figure 3, the simulations conducted at relatively large time-steps produced an oscillatory error profile. This behavior is indicative of simulations conducted above Δt_{max}, where the discrete and continuum governing equations are mathematically inconsistent. Figure 1 also implies that time and space errors do not interact below Δt_{max}, but instead are additive linear functions for the total discretization error. In contrast, Figure 3 indicates that these errors interact non-linearly when they are of comparable magnitude. Fortunately, this behavior is localized near Δt_{max}. To account for these interactions, *verification-controller limits can not be precise*, rather they should be general, conservative guidelines for the a-priori separation of discretization errors.

Another, alternative presentation of this problem's convergence profiles is shown in Figure 4, where the total numerical error is plotted verses the CPR_s. In this logarithmic plot, the slope of each integrator's error profile is minus one. This error-reduction rate is expected because the $CPR_s \propto 1/(\Delta t)^q$ as defined in Equation 8. This error-reduction rate relative to CPR_s is an alternative verification of each integrator. While the error-profile slopes in Figures 3 and 4 are different, other characteristics of their convergence histories are

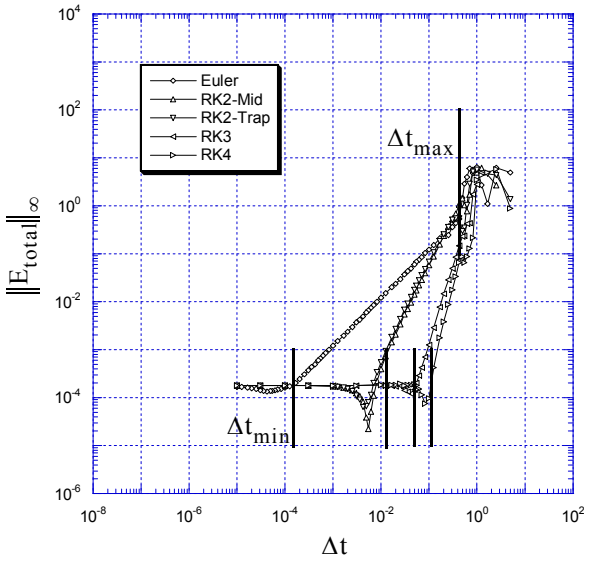

Figure 3: Temporal Convergence History With Constant Spatial Error; $N_c = 1600$; Total Error vs. Time-Step.

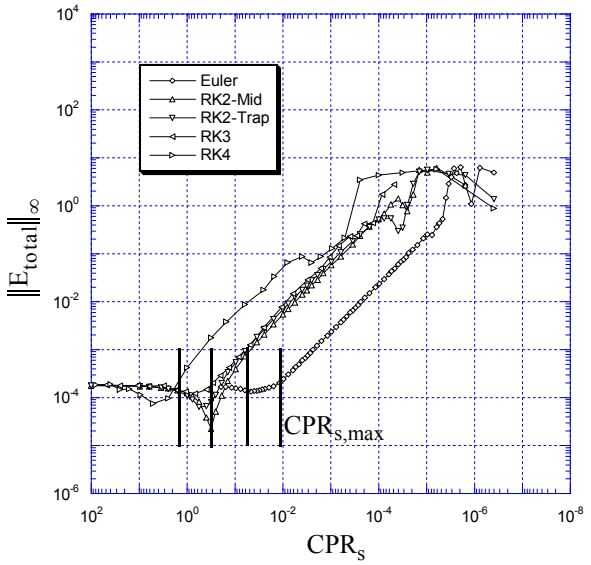

Figure 4: Temporal Convergence History With Constant Spatial Error; $N_c = 1600$; Total Error vs. CPR_s.

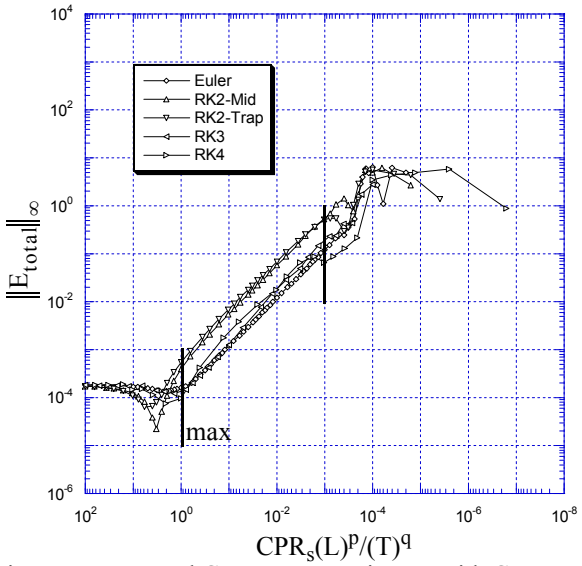

Figure 5: Temporal Convergence History With Constant Spatial Error; $N_c = 1600$; Total Errors vs. $CPR_s L^p/T^q$.

similar. For each integrator, the error near the start of asymptotic regimes is nearly coincident at $L_\infty \approx 10^{-1}$. As the time-step is refined, the error profiles asymptote to the identical, constant spatial error at $L_\infty \approx 2 \times 10^{-4}$.

While an error profile's slope can be used to verify a numerical method, the pertinent feature of these profiles for verification controllers are the asymptotic-regime's bounds. In Figure 4, $CPR_{s,\,min}$ and $CPR_{s,\,max}$ are unique for each integrator. The full extent of each regime, however, is comparable. The span of $CPR_{s,\,min}$ and $CPR_{s,\,max}$ is about three decades except for RK4. This limitation appears as a difficulty in initiating the asymptotic threshold, which may be expected for any higher-order method. The CPR_s appears to be more practical than time-steps for the a-priori separation of discretization errors; while the algorithmic dependence of $CPR_{s,\,max}$ is confirmed in Figure 4, the extent of the asymptotic regime's is similar for each integrator.

In Figure 5, the total numerical error is plotted verses a dimensional variant of CPR_s, which is easily derived from Equation 8: $CPR_s(L)^p/(T)^q$. The slope of each error profile is minus one, which represents the third example of verification in this report. The start and exit of each integrator's asymptotic regime are also similar. Indeed, discretization errors appear to decouple when $CPR_s(L)^p/(T)^q \approx 10^0$. The extent of each integrator's asymptotic regime is also comparable at about three decades. The dimensional variant of the CPR_s appears to be more practical than time-steps for the a-priori separation of errors; the bounds and extent of each integrator's asymptotic regime in Figure 5 are similar.

A fourth presentation of the demonstration problem's error profiles is shown in Figure 6, where the total numerical error is plotted verses the DER_s. In this plot, the slope of each integrator's error profile is minus one because the $DER_s \propto 1/(\Delta t)^q$ as defined in Equation 6. This error-reduction rate relative to DER_s is the fourth example of verification presented in this report.

More importantly, because the convergence profiles are nearly identical in Figure 6, the DER_s appears as a similarity variable for separate verification. At the start of each regime, $DER_{s,\,min}$ is nearly coincident, except for the highest-order integrator which requires a lower starting time-step. At the regime exit, $DER_{s,\,max}$ is also nearly coincident, but there is a slight variation in error profiles between the even and odd-ordered integrators. The even-ordered methods exhibit a more pronounced and slightly broader interactive region around Δt_{max}. In contrast, the odd-ordered methods smoothly transition from temporal to spatial error as the time-step is refined.

The convergence profiles in Figure 6 also support the contention that the DER_s provides a universal constant for separating discretization errors. By definition, the DER_s is unity when the temporal and spatial errors are equivalent. The total numerical error is dominated in Figure 6 by a single error source when the DER_s varies by one or more orders-of-magnitude. Indeed, the non-linear interactive region between two error sources appears to be conservatively bound by $DER_s \approx 10^{\pm 1}$. When $DER_s \geq 10^1$, spatial error dominates the total numerical error. Conversely, when $DER_s \leq 10^{-1}$, the total error is dominated by temporal error. Reduced-ansatz equations, thus, can only be solved accurately

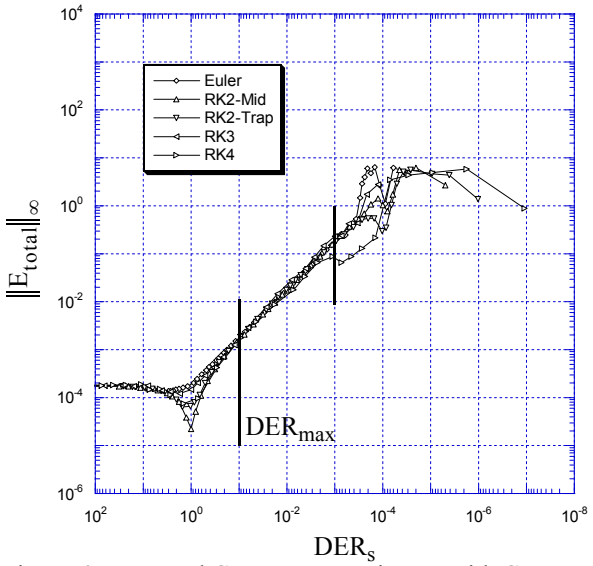

Figure 6: Temporal Convergence History With Constant Spatial Error; $N_c = 1600$; Total Error vs. DER_s.

when discretization errors differ by at least an order-of-magnitude, as codified by $DER_{max} \approx 10^{-1}$.

As discussed above and implied within each figure of this report, minimizing the spatial discretization error may broaden the separate-temporal asymptotic regime. This effective but heuristic strategy to produce pure temporal error, however, can be made precise through the proper use of verification-controllers.

Summary

This report proposes and demonstrates verification controllers. These novel numerical tools can be used to ensure the accuracy and enhance the efficiency of separate time and space convergence studies by decoupling discretization errors. These new tools are algebraic constraints on time-steps and grid-spacings that must be satisfied concurrent with the convergence-study simulations. Two verification controllers are presented: the discretization-error ratio (DER) and the convergence-power ratio (CPR).

Temporal convergence studies were then conducted to assess the verification-controller limits, CPR_{max} and DER_{max}. The CPR_s appears to be more practical than time-steps for the a-priori separation of discretization errors; while the algorithmic dependence of $CPR_{s,\,max}$ is confirmed, the extent of the asymptotic regime's is similar for each integrator. For the dimensional variant of the CPR_s, both the bounds and the extent of the asymptotic regimes are similar for each integrator. The DER was shown to be a similarity variable for separate verification as the convergence histories coalesced onto a single error profile. The DER also implied a universal constant for decoupling errors; accurate separate verification analyses require that discretization errors differ by at least one order-of-magnitude.

While the theoretical foundation and practical utility of verification controllers were explored, the application of these new tools was limited in this initial report. Additional test problems, particularly for more complex numerical PDE solvers and a variety of test problems, are warranted. An investigation into the combined use of verification controllers and CFL constraints, often required for algorithmic accuracy and stability, is also suggested; both of these numerical tools are algebraic constraints on the time-step and grid-spacing that must be satisfied concurrent with the numerical simulation.

Acknowledgement

This work was performed by the Los Alamos National Laboratory, which is operated by the University of California for the U. S. Department of Energy under contract W-7405-ENG-36. The helpful discussions of James R. Kamm are gratefully acknowledged.

References

1) Twizell, E. H., Computational Methods for Partial Differential Equations, Halsted, NY, 1984.

2) Evans, G., Blackledge, J. M. and Yardley, P., Numerical Methods for Partial Differential Equations, Springer, NY, 2000.

3) Roache, P. J., Verification and Validation in Computational Science and Engineering, Hermosa, Albuquerque, NM, 1998.

4) Oberkampf, W. L. and Trucano, T. G., "Verification and Validation in Computational Fluid Dynamics," Sandia National Laboratory, SAND-2002-0529, 2002.

5) Knupp, P. and Salari, K. Verification of Computer Codes in Computational Science and Engineering, Chapman & Hall/CRC, Boca Raton, FL, 2002.

6) Oberkampf, W. L., Trucano, T. G. and Hirsch, C., "Verification, Validation and Predictive Capability in Computational Engineering and Physics," Sandia National Laboratory, SAND-2003-3769, 2003.

7) Kamm, J. R., Rider, W. J. and Brock, J. S., "Consistent Metrics for Code Verification," Los Alamos National Laboratory, LA-UR-02-3794, 2002.

8) Kamm, J. R., Rider, W. J. and Brock, J. S., "Combined Space and Time Convergence Analysis of a Compressible Flow Algorithm," AIAA Paper, AIAA-2003-4241, 2003. (Los Alamos National Laboratory, LA-UR-03-2628, 2003.)

9) Warming, R. F. and Hyett, B. J., "The Modified Equation Approach to the Stability and Accuracy Analysis of Finite-Difference Methods," *Journal of Computational Physics*, Vol. 14, pp. 159-179, 1974.

10) Griffiths, D. F. and Sanz-Serna, J. M., "On the Scope of The Method of Modified Equations," *SIAM Journal on Scientific and Statistical Computing*, Vol. 7, pp. 994-1008, 1986.

11) Villatoro, F. R. and Ramos, J. I., "On the Method of Modified Equations: Asymptotic Analysis of the Euler Forward Difference Method," *Applied Mathematics and Computations*, Vol. 103, pp. 111-139, 1999.

12) Ascher, U. M. and Petzold, L.R., Computer Methods for Ordinary Differential Equations and Differential-Algebraic Equations, SIAM, Philadelphia, PA, 1998.

13) Reddy, J. N., An Introduction to the Finite Element Method, McGraw-Hill, New York, NY, 1984.

14) Brock, J. S., "Discretization Errors for Separate-Verification Analyses," Los Alamos National Laboratory, LA-UR-03-2618, 2003.